

RESEARCH

Open Access



# Numerical and Empirical Models for Service Life Assessment of RC Structures in Marine Environment

Xuandong Chen<sup>1</sup>, Yang Ming<sup>1</sup>, Feng Fu<sup>1,2\*</sup>  and Ping Chen<sup>1</sup>

## Abstract

The service life prediction of reinforced concrete (RC) structures in marine environment is essential in structural repair and health monitoring. In this paper, a numerical model for predicting the service life of reinforced concrete is first developed which considering the time-varying boundary of chloride concentration, critical chloride concentration and density of corrosion current. Based on the model, the effects of water–cement ratio, reinforcement diameter, concrete cover thickness and critical chloride ion concentration on the service life and deterioration duration of RC structures are investigated. The key factors affecting the service life of reinforced concrete structures are determined. More importantly, based on regression analysis, a new simplified empirical model for predicting the service life of RC structures is also developed. It provides a fast assessment tool for practical engineers. Both the numerical model and empirical model validated are suitable for practical engineering applications. The results show that with the increase of water–cement ratio, the service life of reinforced concrete structure decreases exponentially. And with the increase of the thickness of the concrete cover, the service life, deterioration duration, and safety reserve increase linearly. However, the influence of the diameter of the reinforcing bar on the service life can be ignored.

**Keywords:** service life prediction, RC structures, chloride diffusion, critical chloride value, corrosion current density

## 1 Introduction

Reinforced concrete (RC) structures are widely used in normal construction projects, such as tall buildings (Fu, 2018, 2021) and bridges (Fu, 2015, 2016) offshore bridges, subsea tunnels, and harbour projects (Pillai et al., 2019; Xu et al., 2019), and for these types of projects, chloride ingress due to marine environment is one of the main factors causing the corrosion of steel bars (Chang et al., 2020; Marks et al., 2015). However, serious corrosion of steel bars causes the deterioration of structural capacity, causing serious challenges to the durability of RC structures (Alexander & Beushausen, 2019). Therefore,

for marine projects, predicting the service life of the RC structure in marine environment has become an important design task for design engineers. The accurate prediction enables effective health monitoring and timely retrofitting of marine projects in their service life (Bouteiller et al., 2016; Dhandapani et al., 2018). Even for projects under construction, service life prediction can provide important guidelines for designers.

Chloride ingress is particularly problematic to concrete (Nogueira et al., 2012; Shaikh, 2018). Driven by the concentration difference, chloride ions and oxygen in the marine environment diffuse into the interior of concrete through its pores. Unfortunately, once the chloride concentration on the steel surface reaches the critical value, the passivation film on the steel surface will be destroyed. Consequently, the steel reinforcement members encased are subject to corrosive damages (Guo et al., 2004). This erosion of the steel can cause a reduction in

\*Correspondence: feng.fu.1@city.ac.uk

<sup>1</sup> College of Civil Engineering and Architecture at Guilin University of Technology, Guilin 541004, China

Full list of author information is available at the end of the article  
Journal information: ISSN 1976-0485 / eISSN 2234-1315

the RC structures' ability to resist tensile stresses. Hence, chloride ingress induced reinforcement corrosion is one of the main factors affecting the durability of concrete structures and at present, many scholars have carried out extensive research on this issue. Stambaugh et al. (2018) used the critical value of chloride ion concentration on the surface of steel bars as the service life assessment standard and studied the service life of RC structures in marine environments under different circumstances such as the location and the mix ratio (Jung et al., 2018; Khanzadeh-Moradillo et al., 2015; Mir et al., 2019). However, they assumed that the chloride ion concentration on the concrete surface was constant and did not consider the time-varying characteristics of the chloride ion concentration on the surface (Huan et al., 2015; Yang et al., 2017). Muthulingam et al., (2014) established a service life prediction model by considering the influence of wet-heat-diffusion coupling and the time-varying characteristics of the chloride concentration at the boundary. However, the model requires too many input parameters, so it is not practical. It can only predict the moment when the steel bar begins to rust, but it cannot predict when the RC structure will fail, that is, the failure life. Cao et al. (2014) and Zhu et al. (2017; Zhang et al., 2019) established a mechanical model to predict the service life of RC structures. It is based on analysis of the corrosion mechanism of steel bars considering the thickness of concrete cover (Enright & Frangopol, 1998), the critical value of the chloride concentration (Bastidas-Arteaga et al., 2009; Enright & Frangopol, 1998), and the chloride diffusion coefficient (Pack et al., 2010). Zheng et al. (2009) also developed a numerical model to assess the influence of ITZ on the steady-state chloride diffusion. Based on the finite difference method of Crank Nicolson, Song et al. (2009) and Petcherdchoo et al. (2015) studied the effect of retrofitting agents on the service life of RC structures. Jones et al. studied the effectiveness of using filler to repair concrete cracks on prolonging the service life of RC structures. These studies show that when micro-cracks appear on the surface of concrete, repair agents can greatly prolong the service life of RC structures. Furthermore, Attari et al. established a failure probability model for RC structures. In these studies, when the failure probability reached 10%, the RC structure is considered to have reached the service life, and the cracks in the RC structure have reached an acceptable limit.

Although many service life prediction models for RC structures have been developed, there are still many challenges that have not been resolved. For example, most of the existing models only use the critical chloride concentration as the basis for predicting service life. However, the critical chloride concentration is only the indication of beginning of steel bar corrosion (Zhao, et al., 2011b).

The life cycle performance of reinforced concrete structures after reinforcement corrosion is rarely concerned in the existing service life models (Pan et al. 2015). Most importantly, most of the existing models calculated the service life of RC structures by solving complex partial differential equations, which greatly increases the computational cost and is difficult to use in practical engineering. Moreover, the chloride concentration at the boundary of concrete is time-dependent rather than constant, which will directly affect the distribution of chloride in concrete.

Therefore, the focus of this research is to address above issues. The main purpose of this research is to establish a practical models for practising engineers, allowing them to use easily quantifying engineering parameters for predicting the service life of RC structures. Firstly, a complex numerical model to predict the service life of RC structures is established by diffusion-corrosion theory. The model verifications show that both the chloride ion concentration and service life predictions agree well with the measured values. Secondly, based on proposed model, the influence of factors such as the thickness of the cover, the water-cement ratio, the critical value of chloride ion concentration, and the diameter of the reinforcement on the service life of the RC structure are analysed. Finally, through a two-stage regression simulation of the service life of RC structures under 300 different conditions, an empirical model for predicting the service life of RC structures is established. By comparing with the numerical simulation results, the empirical model is in good agreement with the numerical model. The models proposed in this paper provide important theoretical support for life assessment of existing projects and optimization of service life design of projects to be built.

## 2 Theoretical Background

### 2.1 Chloride Diffusion Model

After decades of theoretical and experimental research by many scholars (Hobbs, 1999; Wang et al., 2018, 2019; Zeng, 2007; Zheng et al., 2018), the diffusion of chloride ions in concrete in line with Fick's second law has become a widely used. And the governing equation for the diffusion of chloride ions in concrete is expressed as:

$$\frac{dc}{dt} = \frac{\partial c}{\partial x} \left( D_c \frac{\partial c}{\partial x} \right) + \frac{\partial c}{\partial y} \left( D_c \frac{\partial c}{\partial y} \right), \quad (1)$$

where  $c$  is chloride ion concentration (mass ratio of chloride ion to concrete, %),  $D_c$  is chloride ion diffusion coefficient ( $m^2/s$ ), respectively.

### 2.1.1 Chloride Diffusion Coefficient

It can be seen from Eq. (1) that the chloride ion diffusion coefficient is a key parameter that determines the diffusion rate of chloride ions in concrete. The chloride ion diffusion coefficient is not only related to the factors such as concrete types, pore structure, water–cement ratio, hydration degree, etc., but also to the external environment, such as temperature (Bažant & Najjar, 1972), humidity (Muthulingam & Rao, 2014), current time (Zeng, 2007). However, to simplify it, in this paper, the chloride ion diffusion coefficient is calculated with only considerations of the effects of water–cement ratio, temperature, humidity, and aging. Its expression is (Muthulingam & Rao, 2014; Chen et al., 2019):

$$D_c = \underbrace{\frac{2 \times \varphi_p^{2.75} D_p}{\varphi_p^{1.75} (3 - \varphi_p) + n(1 - \varphi_p)^{2.75}}}_{\text{Water - cement ratio}} \cdot \underbrace{\exp \left[ \frac{U_c}{R} \left( \frac{1}{T_{ref}} - \frac{1}{T} \right) \right]}_{\text{Temperature}} \cdot \underbrace{\left[ 1 + \frac{(1 - h)^4}{(1 - h_c)} \right]^{-1}}_{\text{Humidity}} \cdot \underbrace{\left( \frac{t_{ref}}{t} \right)^m}_{\text{Curing age}}, \quad (2)$$

where  $U_c$  is the activation energy for chloride ion diffusion,  $t_{ref}$  is the average exposure time,  $R$  is the gas constant,  $T_{ref}$  is the absolute ambient temperature,  $h$  is humidity,  $h_c$  is critical humidity (0.75),  $D_p$  is the diffusion coefficient of chloride ions in water,  $n$  is an empirical constant (using 14.44 as reference (Du, et al., 2014)),  $m$  is the time decay index, and  $f_p$  is the porosity of the cement slurry, respectively.  $f_p$  can be expressed as (Chen, et al., 2021):

$$\varphi_p = \frac{w/c - 0.17\alpha}{w/c + 0.32}, \quad (3)$$

where  $\alpha$  is the degree of hydration of cement slurry, and  $w/c$  is water to cement ratio, respectively. The value of the degree of hydration of cement slurry  $\alpha$  in formula (3) can be calculated by:

$$\alpha = 1 - \exp(-3.15 \times w/c). \quad (4)$$

### 2.1.2 Surface Chloride Ion Concentration

The surface chloride ion concentration on the concrete is another key factor affecting the chloride ion concentration inside the concrete. In the numerical solution, the surface chloride ion concentration is also called the boundary condition. In the marine environment, chloride ions are transmitted to the surface of offshore engineering concrete structures through the flow of the air, and then diffuse into the concrete through the pores of the concrete (Yang, et al., 2017). Fig. 1 shows statistics of chloride ion concentration on the surface of marine engineering concrete structures in different coastal areas by different scholars (Huan et al., 2015; Meira et al., 2007;

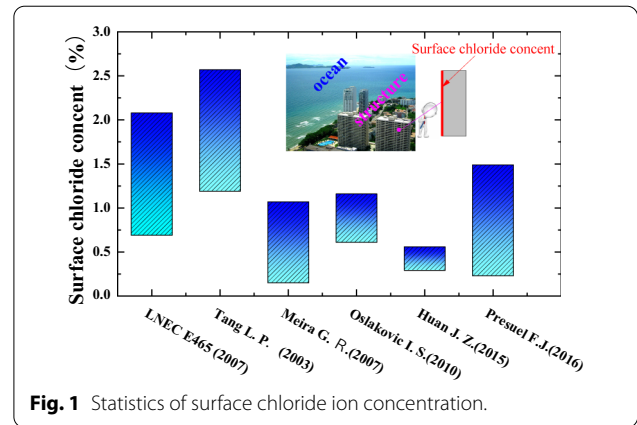


Fig. 1 Statistics of surface chloride ion concentration.

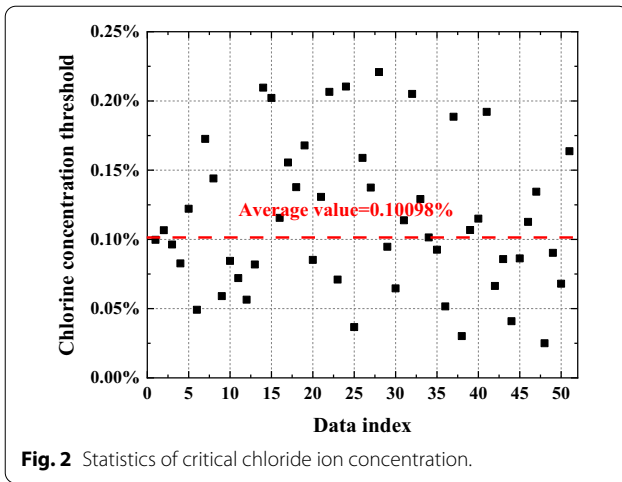
Stipanovic Oslakovic et al. 2010). It can be seen from Fig. 1 that the surface chloride ion concentration ranges from 0.1% to 2.5%. There are many factors that affect the chloride ion concentration on the concrete surface, such as temperature, humidity, cement type, and water-binder ratio. Yang et al. (2019) obtained the regression equation of surface chloride ion and time function through regression analysis of 372 sets of surface chloride ion concentration data. It is worth noting that Eq. (5) is based on the test results of ordinary Portland concrete. Therefore, Eq. (5) is only applicable to ordinary Portland concrete, but not to special concrete, such as fly ash concrete, slag concrete, etc.:

$$C_s(t) = \frac{5.3t}{1 + 0.7047t} \times \frac{w}{c}. \quad (5)$$

## 2.2 Rebar Corrosion

### 2.2.1 Critical Chloride Ion Concentration

Chloride ions accumulate on the surface of the steel bars over the time. When the concentration of chloride ions on the surface of the steel bars reaches certain value, the steel bar begins to corrode. This value is called the critical chloride ion concentration. The critical chloride ion concentration indicators include free chloride ion concentration, total chloride ion concentration, and the ratio of free chloride ion concentration to hydroxide concentration (Cao et al., 2019). In this paper, the total chloride ion concentration is used as an index to measure the critical chloride ion concentration. Due to the differences in the measuring methods and the discrete type of concrete materials, the critical chloride ion concentration



cannot be determined at present. The critical chloride ion concentration currently reported is between 0.079% and 0.2% (Zhao, et al., 2011a). The critical chloride ion concentration from 51 existing literature is collected in this paper. Their statistical distribution is shown in Fig. 2. From Fig. 2, the critical chloride ion concentration distribution is relatively scattered. Therefore, the mean value of 0.10098% is used in this paper as the critical chloride ion concentration.

**2.2.2 Corrosion Current Density**

The chloride ion concentration is not constant across the whole volume of concrete. The chloride ion concentration near the erosion surface is high, and the chloride ion concentration away from the erosion surface is low (Pan, et al., 2015). Therefore, the chloride ion concentration on the surface near the cover first reaches the critical chloride ion concentration, and the passivation film was damaged (Li, et al., 2019). Research in literature (Cao, 2014) shows that there is a potential difference between the active area formed after the passivation film on the steel bar is damaged and the inert area where the passivation film is not damaged, and a macroscopic electrochemical corrosion is formed. At the same time, there is also a micro-corrosion current, the total corrosion current density can be expressed as (Zhu & Zi, 2017):

$$i_{corr} = i_{mic} + i_{mac}, \tag{6}$$

where  $i_{corr}$  is the total corrosion current density,  $i_{mic}$  is the micro-battery corrosion current density, and  $i_{mac}$  is the macro-battery corrosion current density, respectively.

At present, many empirical, theoretical, and numerical models have been established to calculate the corrosion current density of steel bars. In this paper, the Probabilistic mode of Papakonstantinou et al. (2013) is adopted, with the expression:

$$\ln 1.08i_{corr} = 7.89 + 0.7771 \ln (1.69c_t) - \frac{3006}{T} - 0.000116R_c, \tag{7}$$

where  $i_{corr}$  is the corrosion current density,  $c_t$  is total chloride ion concentration, and  $R_c$  is resistance of the concrete cover, respectively.

The empirical formula given by Liu et al. (1998) for resistivity of concrete cover is:

$$\ln R_c = 8.03 - 0.549 \ln (1 + 1.69c_t). \tag{8}$$

**2.3 Determination of Service Life**

In general, when the chloride ion concentration on the surface of the steel bar reaches the critical chloride ion concentration, the marine engineering concrete structure is considered to have reached the service life. The limit state function at this stage can be expressed as:

$$G_1(c, t) = C_{cri} - C(\max, t), \tag{9}$$

where  $G_1(c, t)$  is the limit state function,  $c_{cri}$  is the critical chloride ion concentration, and  $c(\max, t)$  is the maximum chloride ion concentration on the steel bar surface at the ingress time of  $t$ , respectively.

It is worth mentioning that when the maximum chloride ion concentration on the surface of the steel bar reaches the critical chloride concentration, the offshore engineering concrete structure does not fail, and only the steel bars begin to rust (Zhao, et al., 2011a; Zhao et al., 2016). The radial expansion stress is developed during the corrosion process. When the radial expansion stress starts to cause damage to the concrete cover, the cover will crack and peel, and the structure will fail (Zhao, et al., 2011b). In this paper, it is called the structural failure life. The limit state function can be expressed as:

$$G_2(\lim, t) = \rho_{cr} - \rho(\lim, t), \tag{10}$$

where  $\rho_{cr}$  is the steel rebar erosion rate at failure of the structural concrete (%), it is calculated as:

$$\rho_{cr} = \frac{2(\delta_1 + \delta_2)}{r_0}, \tag{11}$$

where  $\delta_1$  is the depth of rust generated by filling the pores in the transition zone between the steel bar and concrete at the interface between the corrosion products is 12.5  $\mu\text{m}$ ;  $\delta_2$  is the depth of rust producing radial pressure, it is worked out based on the theory of thick-walled cylinders (Xu, et al., 2019b), and can be expressed as:

$$\delta_2 = \frac{r_0}{E_c} \left[ \frac{(r_0 + c)^2 + r_0^2}{(r_0 + c)^2 - r_0^2} + \nu_c \right] \cdot \left[ 0.3 + 0.6 \frac{c}{2r_0} \right] \cdot f_t, \tag{12}$$

where  $r_0$  is the reinforcement radius (mm),  $\nu_c$  is the Poisson's ratio of the concrete cover,  $E_c$  is elastic modulus of concrete (MPa), and  $f_t$  is tensile strength of concrete (MPa), respectively.

$\rho(\text{lim}, t)$  is the corrosion rate of steel bars at time  $t$  (%). According to Faraday's law, the distribution of corrosion depth  $u_d(\theta, t)$  around steel bars can be expressed as (Alexander & Beushausen, 2019; Chen et al., 2019; Zhang et al., 2019):

$$u_d(\theta, t) = \int_{t_c}^t 0.0116 \cdot i_{\text{corr}}(\theta, t) dt. \tag{13}$$

The mass loss of rebar can be expressed as:

$$M_S = \rho_s \int_0^{2\pi} u_d(\theta, t) d\theta, \tag{14}$$

where  $\rho_s$  is the density of the rebar ( $\text{kg}/\text{m}^3$ ).

So:

$$\rho(\text{lim}, t) = \frac{\rho_s \int_0^{2\pi} u(\theta, t) d\theta}{\rho_s \cdot \pi \cdot r_0^2} \times 100\% = \frac{\int_0^{2\pi} u(\theta, t) d\theta}{\pi \cdot r_0^2} \times 100\%. \tag{15}$$

In summary, the flowchart of service life prediction for RC structures is shown in Fig. 3.

### 3 Numerical Model Validation

The numerical model proposed in this paper comprises two stages modelling. The first stage is the diffusion of chloride ions, and the second stage is the corrosion of steel bars. Therefore, the model verification in this section is also divided into two aspects: chloride ion diffusion verification and service life. The parameters used in the simulation are listed in Table 1. In the process of numerical simulation, the finite difference method (FEM) is adopted to solve the chloride ion diffusion equation (Eq. 1) to obtain the distribution of chloride ion concentration in concrete. Once the chloride concentration on

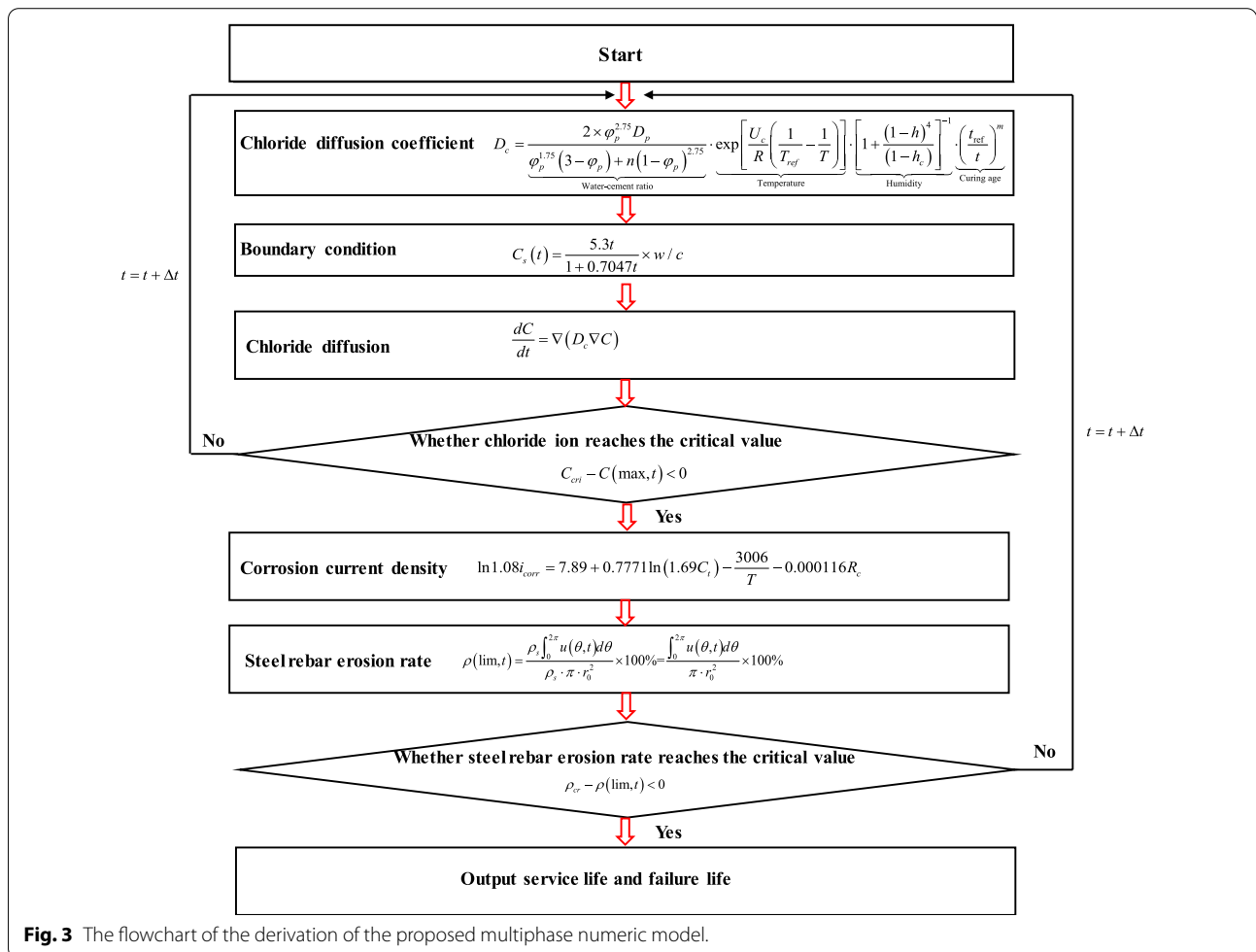


Fig. 3 The flowchart of the derivation of the proposed multiphase numeric model.

**Table 1** Numerical simulation parameters.

Symbol	Parameter value	Mean
$U_c$	44.6 [K J/mol]	The activation energy for chloride diffusion
$t_{ref}$	28 [d]	Reference time of chloride ingress
$R$	8.314 [J/K mol]	The gas constant
$h_c$	0.75 [-]	The critical humidity
$h$	1	Humidity
$D_p$	$1.07 \times 10^{-10}$ [m <sup>2</sup> /s]	The diffusion coefficient of chloride in water
$m$	0.2	The time decay index of chloride diffusion
$\rho_s$	7500 [kg/m <sup>3</sup> ]	The density of the rebar
$T_{ref}$	293 [K]	Reference temperature
$\delta_1$	12.5 $\mu$ m	The depth of rust generated by filling the pores
$r_0$	8–13 mm	The reinforcement radius
$E_c$	30 [GPa]	Elastic modulus of concrete
$f_t$	1.43 [MPa]	Tensile strength of concrete
$\nu_c$	0.2	The Poisson's ratio of the concrete
$c$	40–70 mm	Thickness of reinforced concrete cover
$w/c$	0.45, 0.55, 0.65	The water-to-cement ratio

the steel surface reaches the critical chloride concentration, the concrete structure will reach its service life. Secondly, the steel corrosion rate is calculated through Eq. (15). Once the steel corrosion rate reaches the critical steel corrosion rate, the concrete structure will reach its failure life.

### 3.1 Chloride Diffusion Verification

The experimental data of Chalee et al. (2009) will be used to compare with the numerical simulation in this paper. The size of the concrete cube specimen was 200 mm  $\times$  200 mm  $\times$  200 mm, and the water–cement ratio was 0.45, 0.55, 0.65. And the concrete is immersed in seawater, which indicates that the concrete is saturated. Therefore, relative humidity of the concrete is 1 in numerical simulation. In addition, the average value of the external ambient temperature is 293 K. The comparison between numerical simulation results and test results is shown in Fig. 4. Obviously, the chloride concentration curve obtained by numerical simulation is very close to that obtained by experiment, which indicates that the chloride diffusion model is reliable.

### 3.2 Service Life Verification

The service life prediction model proposed in this paper is compared with Moraddllo et al. (2012) and Aruz et al. (Petcherdchoo & Chindapasirt, 2019). The

thickness of the concrete cover is 50 mm and 60 mm, and the water–cement ratio is selected as 0.55. In addition, the concrete is saturated, i.e. the relative humidity is 1. The average temperature of the environment is 293 K. Reinforcement diameter is 10 mm. Fig. 5 shows the comparison of the service life of the three models; it can be seen that the differences in the service life predictions of the three models are small, which indicates that the numerical model established in this paper has a certain degree of reliability.

## 4 Parametric Analysis Using the New Numerical Model

Using the proposed numerical model, intensive parametrical studies are made, which are show as follows.

### 4.1 Influence of Different Water–Cement Ratios

The water–cement ratio for different concrete strength grades is different. However, different water–cement ratio has great influence on the chloride diffusion coefficient and the chloride ion concentration on the concrete surface, especially for the chloride diffusion coefficient (Ishida, et al., 2009). Therefore, the water–cement ratio has a very important influence on the durability of RC structures (Pack et al., 2010). Fig. 6a shows the service life of RC structures in the marine environment as a function of water–cement ratio. It can be seen from Fig. 6a that the water–cement ratio has a very important effect on the service life of the marine engineering concrete structure. For example, when the water–cement ratio is 0.36, the service life is 46.1 years. However, when the water–cement ratio is increased to 0.55, the service life is only 6.3 years. Therefore, in marine engineering, using a low water–cement ratio can effectively increase the service life of the structure. Besides, Fig. 6a also shows the relationship between the deterioration duration and the water–cement ratio. The deterioration duration also decreases exponentially as the water–cement ratio increases. Moreover, as the water–cement ratio increases, the safety reserve decreases more slowly. The larger the water–cement ratio is, the longer the safety reserve period is, and the safety reserve period varies from 5.8 years to 9.8 years. Fig. 6b shows the change of the maximum chloride ion concentration on the surface of the steel bar with time under different water–cement ratios. It can be seen from Fig. 6b that under the same ingress time, as the water–cement ratio increases, the chloride ion concentration gradually decreases. For example, when the water–cement ratio is 0.55, the maximum chloride ion concentration on the surface of the steel bar increased rapidly within 0 to 20 years, and then increased slowly.

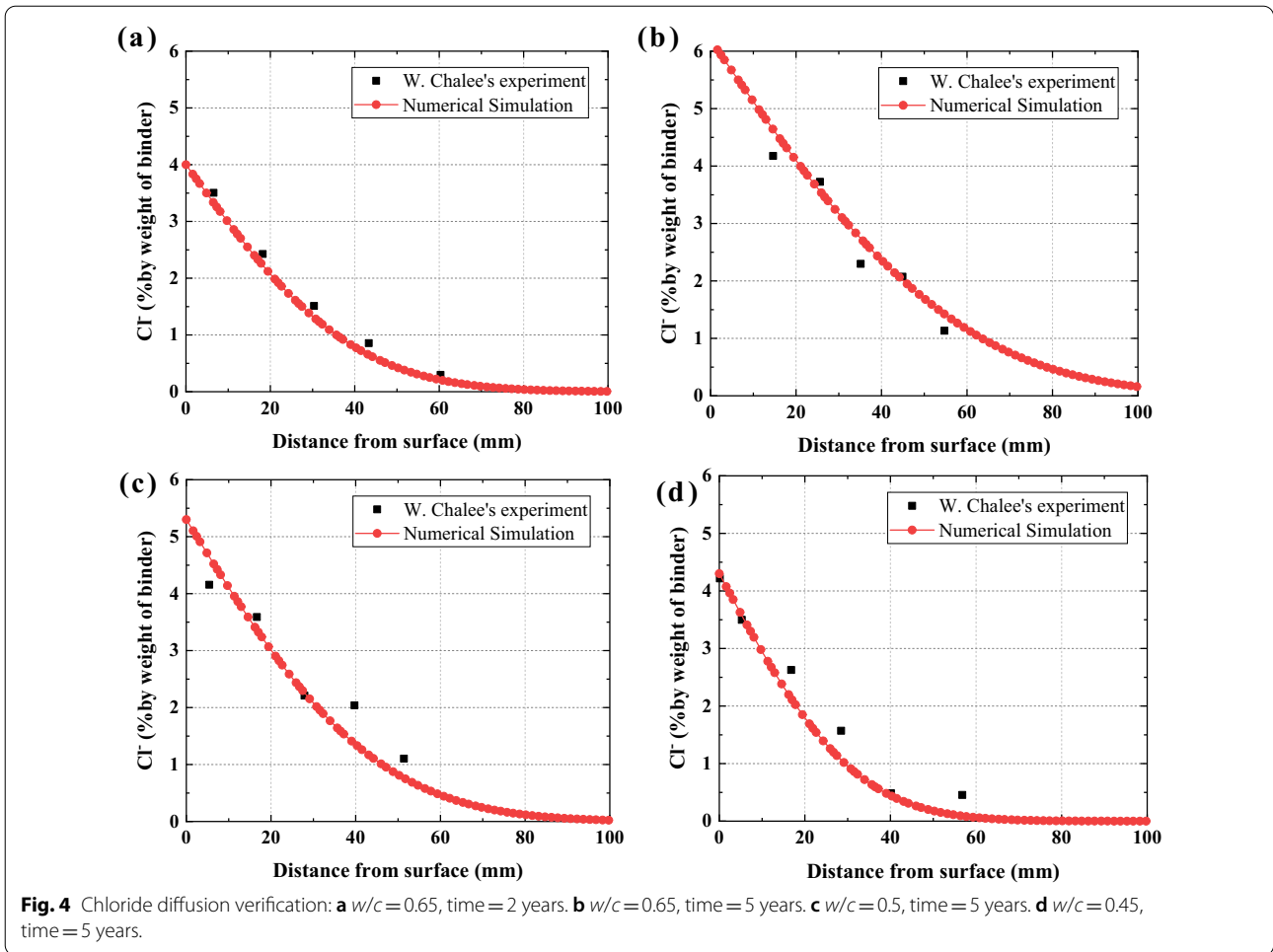


**Fig. 4** Chloride diffusion verification: **a**  $w/c = 0.65$ , time = 2 years. **b**  $w/c = 0.65$ , time = 5 years. **c**  $w/c = 0.5$ , time = 5 years. **d**  $w/c = 0.45$ , time = 5 years.

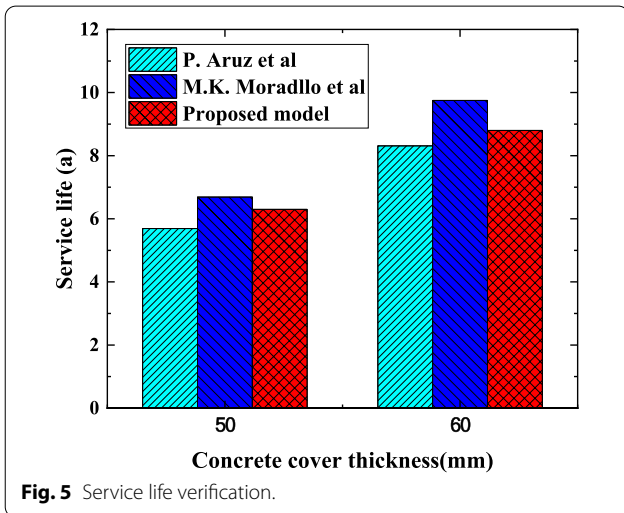


**Fig. 5** Service life verification.

#### 4.2 Thickness of Concrete Cover

The thickness of the concrete cover is an important parameter for structural design. For different environments, the requirements for the thickness of the concrete cover are different in the Code for durability Design of concrete structures. Therefore, it is necessary to study the effect of concrete cover thickness on service life. Fig. 7a shows the values of three indicators of service life, failure life, and safety reserve under different concrete cover thicknesses. It can be seen from Fig. 7a that with the increase of the concrete cover thickness, the service life, deterioration duration and safety reserve all increase. For example, when the thickness of the cover is 40 mm, the service life is only 15.2 years. However, when the thickness of the concrete cover increased to 70 mm, the service life increased to 55.7 years, which was an increase of

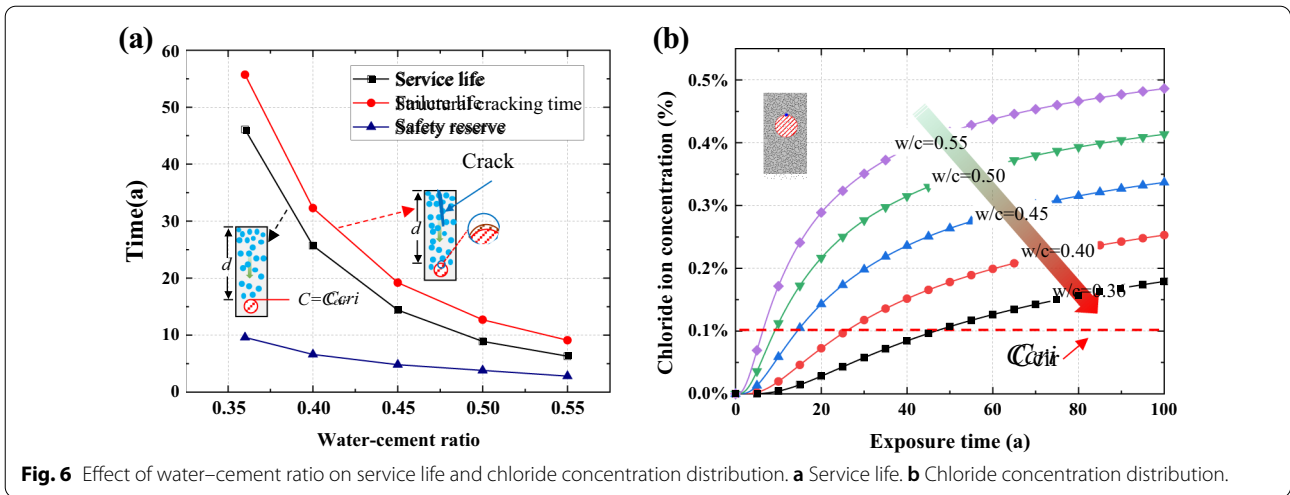


Fig. 6 Effect of water–cement ratio on service life and chloride concentration distribution. a Service life. b Chloride concentration distribution.

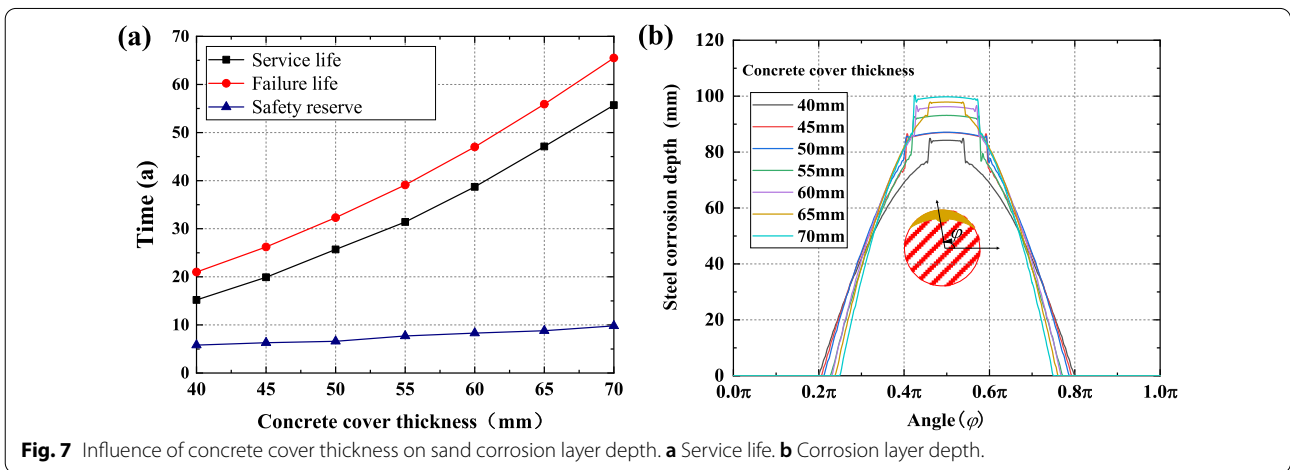


Fig. 7 Influence of concrete cover thickness on sand corrosion layer depth. a Service life. b Corrosion layer depth.

3.67 times compared to the 40 mm thickness of the concrete cover.

Further research found that with the increase of the thickness of the cover, the range of the change in the safety reserve period was small and had a linear relationship with the thickness of the concrete cover. However, deterioration duration increases greatly with the increase of the thickness of the concrete cover. Fig. 7b shows the depth of the corrosion of the steel bar when the cover is cracked under different thicknesses of the concrete cover. It can be seen from Fig. 7b that the corrosion geometric form of the steel bar with different cover thickness is similar, but the peak of the corrosion depth increases with the thickness of the cover and increase. For instance, when the thickness of the concrete cover is 40 mm, the depth of rust is 82.3 μm, however, when the thickness of the concrete cover is 70 μm, the depth of rust is 100.4 μm. Moreover, the corrosion depth curve of the steel bar in this paper is similar to the numerical model of Jinxia (Xia

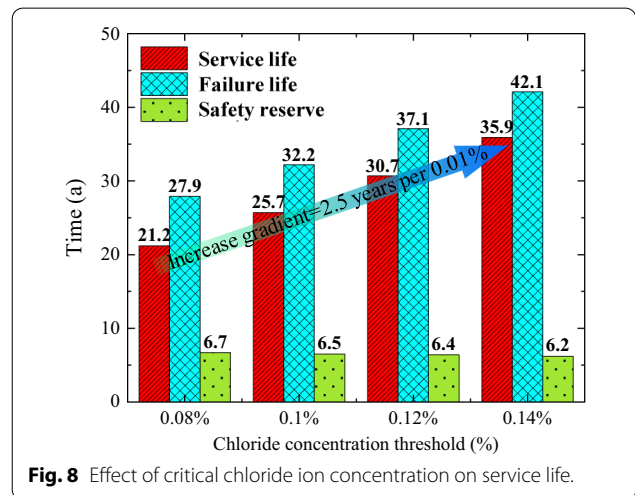


Fig. 8 Effect of critical chloride ion concentration on service life.

et al., 2019), and this corrosion curve is similar to the corrosion mode of the entire steel bar observed through field exposure test experiments (Kessler et al., 2016; Poupard et al., 2006; Sun et al., 2002).

### 4.3 Influence of Critical Chloride Ion Concentration

The critical chloride ion concentration is another important factor affecting the corrosion of steel bars. For different types of steel bars, cement types and service environments, the critical chloride ion concentration is not same. The critical chloride ion concentration obtained by many scholars has a very large value (Cao, et al. 2019, Zhang, et al. 2019). Therefore, in this section, the influence of different critical chloride ion concentrations on the service life of RC structure is studied with a water–cement ratio of 0.4. As shown in Fig. 8, as the critical chloride ion concentration increases, both the service life and the deterioration duration of the RC structure increase. More importantly, it turns out that the critical chloride ion concentration has a linear relationship with the service life, which is consistent with the results of Muthulingam et al. (2014). For instance, for every 0.01% increase in the critical chloride ion concentration, the RC structural service life increases by 2.5 years.

### 4.4 Effect of Rebar Diameter

For different types and functions RC structures, the rebar diameter in the RC structure is also different. Therefore, it is of great significance to study the impact of the rebar diameter on the service life of marine RC structures. Fig. 9 shows a histogram of the service life, failure life, and safety reserve of marine RC structures in the range of rebar diameters from 16 to 26 mm. It can be seen from Fig. 9 that the influence of the rebar diameter on the service life could be ignored (e.g., the difference between the maximum and the minimum service life for different rebar diameter is only 0.5 year).

This is mainly because the service life mainly depends on the critical chloride concentration and thickness of concrete cover. Additionally, as the diameter of the steel bar increases, the deterioration duration and safety reserve both increases, but the upward trend is also slight. For example, when the rebar diameter is 16 mm, the deterioration duration and safety reserve are 32.7 years and 6.4 years, respectively. And when the rebar diameter changes to 26 mm, the deterioration duration and safety reserve of the RC structure are 34.6 years and 8.1 years, respectively. Fig. 9 also shows the corrosion rate of steel bars when the structure fails under different the rebar diameters. It is worth mentioning that as the rebar diameter increases, the corrosion rate of the rebar decreases significantly. For example, when the rebar diameter is 16 mm, the corrosion rate of the rebar is 0.382%; however, when the rebar diameter is 26 mm, the rebar corrosion rate is only 0.241%.

## 5 A Simplified Empirical Model for Service Life Prediction

According to the discussion in Sect. 4, it can be seen that the rebar diameter has a small effect on the service life of the structure. And the thickness of the cover, the water–cement ratio and the critical chloride ion concentration all have significant impact on the service life of the concrete structure. The cover thickness and water–cement ratio are important parameters in engineering design. Therefore, in this paper, 300 groups RC structures with different water–cement ratios, concrete cover thickness are simulated to predict their service life. These 300 groups of data are divided into two categories: first, the thickness of the cover—40 mm, 45 mm, 50 mm, 55 mm, 60 mm, 70 mm, and the water–cement ratios 0.36, 0.40, 0.50, and 0.55. Second, the cover thickness is 65 and the water–cement ratio is 0.45 as a control group. A two-stage data fitting and regression analysis method are used to establish an empirical service life prediction model. In the first stage, the functional representing the relationship between the thickness of the cover and the service life is obtained through regression analysis, as shown in formula (16), where  $A$  and  $B$  is the undetermined coefficient related to water–cement ratio. In the second stage, through regression analysis, the relationship between the undetermined coefficients  $A$  and  $B$  and the water–cement ratio is obtained, as shown in formula (17):

$$f(w/c, cd) = A + B \times cd, \tag{16}$$

where  $A$  and  $B$  are fitting parameters;  $w/c$  is water–cement ratio;  $cd$  is the thickness of concrete cover:

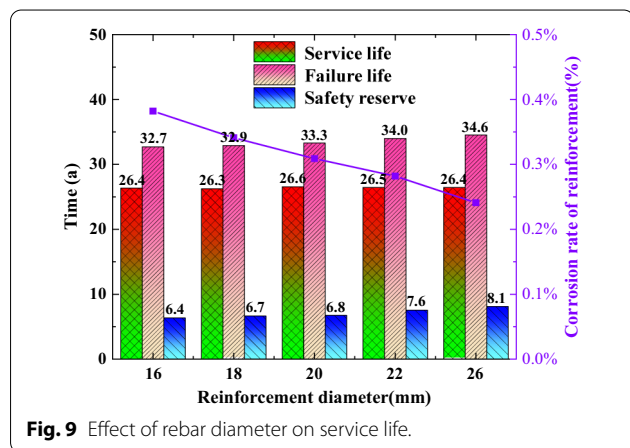
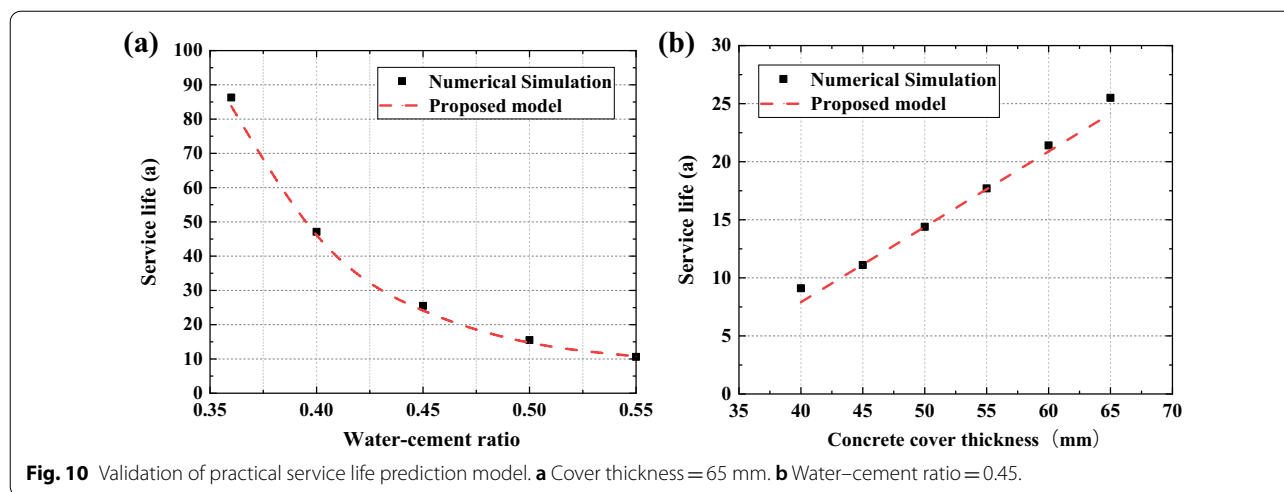


Fig. 9 Effect of rebar diameter on service life.



$$f(wc, cd) = -4.0 + \exp\left(-\frac{326w/c}{19} + 10.364\right) + \left[\frac{2}{11} + \exp\left(-\frac{137w/c}{8} + 6.945\right)\right] \times cd. \tag{17}$$

However, in the process of numerical simulation, we assume that the ambient temperature is 293 K and the concrete is saturated. Therefore, the applicable condition of formula (17) is saturated concrete with an ambient temperature of 293 K.

Fig. 10 shows the comparison between the service life prediction model proposed in this paper and the numerical simulation results. It can be found that the numerical simulation results are distributed near the prediction model curve, which indicates that the proposed model in this paper is reliable.

### 6 Conclusion

In this paper, both numerical and empirical models for predicting the service life of RC structures in the marine environment are proposed. The proposed numerical analysis model not only considers the service life of RC structures, but also the deterioration duration. Moreover, the effects of water-cement ratio, rebar diameter, concrete cover thickness and critical chloride ion concentration on the service life and deterioration duration of RC structures are comprehensively analysed, and the key factors affecting the service life of RC structures are determined. The following conclusions can be drawn:

- (1) With the increase of water-cement ratio, the service life of RC structure decreases exponentially. When the water-cement ratio is 0.36, the service

- life is 46.1 years. However, when the water-cement ratio is increased to 0.55, the service life is only 6.3 years.
- (2) With the increase of the thickness of the concrete cover, the service life, failure life, and safety reserve all linear increase. Thickness of corrosion layer with different cover thickness is similar, but the peak of the corrosion depth increases with the thickness of the cover increase.
- (3) As the critical chloride ion concentration increases, both the service life and the deterioration duration of the RC structure increase. More importantly, it turns out that the critical chloride ion concentration has a linear relationship with the service life.
- (4) The influence of the rebar diameter on the service life can be ignored. It is worth mentioning that as the rebar diameter increases, the corrosion rate of steel bars decreases significantly.
- (5) Various factors (water-cement ratio, protective layer thickness, rebar diameter, etc.) have a small impact on the safety reserve period. The safety reserve period of RC structure is generally less than 10 years.
- (6) Through regression analysis of 300 sets of simulation data, the proposed empirical forecasting model has good reliability in the service life prediction of RC structures and is suitable for practical engineers.

### Acknowledgements

The authors appreciate the financial supports from the National Natural Science Foundation of China (No. 51968014, 52078509, 51968013), Guangxi Key Laboratory of New Energy and Building Energy Saving Foundation (No. 19-J-21-4, 19-J-21-8), and Guangxi Universities Scientific Research Project (2020KY06029).

### Authors' contributions

XC: writing—original draft preparation, data curation, writing, conceptualization, methodology, investigation. FF: writing—original draft preparation, writing—reviewing and editing, methodology, investigation. PC: validation, software. YM: software, data curation. All authors read and approved the final manuscript.

### Authors' information

Xuandong Chen MSc, lecturer, College of Civil Engineering and Architecture, Guilin University of Technology, Guilin 541004, China; China. Guangxi Key Laboratory of New Energy and Building Energy Saving, Guilin 541004, China; Guangxi Engineering and Technology Center for Utilization of Industrial Waste Residue in Building Materials, Guilin, 541004, China.

Yang Ming, MSc, Engineer, Guangxi Engineering and Technology Center for Utilization of Industrial Waste Residue in Building Materials, Guilin, 541004, China.

Feng Fu, PhD Associate Professor, School of Mathematics, Computer Science and Engineering, City, University of London, London EC1C,0HB U.K. (corresponding author).

Ping Chen PhD, Senior Research Fellow, Guangxi Engineering and Technology Center for Utilization of Industrial Waste Residue in Building Materials, Guilin, 541004, China.

### Funding

National Natural Science Foundation of China (No. 51968014, 52078509, 51968013). Guangxi Key Laboratory of New Energy and Building Energy Saving Foundation (No. 19-J-21-4, 19-J-21-8). Guangxi Universities Scientific Research Project (2020KY06029).

### Availability of data and materials

All data that support the findings of this study are available from the corresponding author upon reasonable request.

### Declarations

### Competing interests

The authors declare no competing interests.

### Author details

<sup>1</sup>College of Civil Engineering and Architecture at Guilin University of Technology, Guilin 541004, China. <sup>2</sup>School of Mathematics, Computer Science and Engineering, City, University of London, London EC1C 0HB, UK.

Received: 21 May 2021 Accepted: 14 January 2022

Published online: 14 February 2022

### References

- Alexander, M., & Beushausen, H. (2019). Durability, service life prediction, and modelling for reinforced concrete structures—Review and critique. *Cement and Concrete Research*, 122, 17–29. <https://doi.org/10.1016/j.cemconres.2019.04.018>
- Bastidas-Arteaga, E., et al. (2009). Probabilistic lifetime assessment of RC structures under coupled corrosion-fatigue deterioration processes. *Structural Safety*, 31(1), 84–96. <https://doi.org/10.1016/j.strusafe.2008.04.001>
- Bažant, Z. P., & Najjar, L. J. (1972). Nonlinear water diffusion in nonsaturated concrete. *Matériaux Et Constructions*, 5(1), 3–20. <https://doi.org/10.1007/BF02479073>
- Bouteiller, V., Marie-Victoire, E., & Cremona, C. (2016). Mathematical relation of steel thickness loss with time related to reinforced concrete contaminated by chlorides. *Construction and Building Materials*, 124, 764–775. <https://doi.org/10.1016/j.conbuildmat.2016.07.078>
- Cao, C. (2014). 3D simulation of localized steel corrosion in chloride contaminated reinforced concrete. *Construction and Building Materials*, 72, 434–443. <https://doi.org/10.1016/j.conbuildmat.2014.09.030>
- Cao, Y., et al. (2019). Critical chloride content in reinforced concrete—An updated review considering Chinese experience. *Cement and Concrete Research*, 117, 58–68. <https://doi.org/10.1016/j.cemconres.2018.11.020>
- Chalee, W., Jaturapitakkul, C., & Chindaprasirt, P. (2009). Predicting the chloride penetration of fly ash concrete in seawater. *Marine Structures*, 22(3), 341–353. <https://doi.org/10.1016/j.marstruc.2008.12.001>
- Chang, W., et al. (2020). Durability and aesthetics of architectural concrete under chloride attack or carbonation. *Materials*, 13(4), 839. <https://doi.org/10.3390/ma13040839>
- Chen, X., et al. (2019). Meso-numerical simulation of service life prediction for marine structures. *Journal of Building Materials*, 22(6), 894–900. <https://doi.org/10.3969/j.jissn.1007-9629.2019.06.009>
- Chen, X., et al. (2021). A multi-phase mesoscopic simulation model for the long-term chloride ingress and electrochemical chloride extraction. *Construction and Building Materials*, 270, 121826. <https://doi.org/10.1016/j.conbuildmat.2020.12.1826>
- Dhandapani, Y., et al. (2018). Mechanical properties and durability performance of concretes with Limestone calcined clay cement (LC3). *Cement and Concrete Research*, 107(March), 136–151. <https://doi.org/10.1016/j.cemconres.2018.02.005>
- Du, X., Jin, L., & Ma, G. (2014). A meso-scale numerical method for the simulation of chloride diffusivity in concrete. *Finite Elements in Analysis and Design*, 85, 87–100. <https://doi.org/10.1016/j.finel.2014.03.002>
- Enright, M. P., & Frangopol, D. M. (1998). Probabilistic analysis of resistance degradation of reinforced concrete bridge beams under corrosion. *Engineering Structures*, 20(11), 960–971. [https://doi.org/10.1016/S0141-0296\(97\)00190-9](https://doi.org/10.1016/S0141-0296(97)00190-9)
- Fu, F. (2015). *Advanced Modeling Techniques in Structural Design*. USA: Wiley. 978-1-118-82543-3.
- Fu, F. (2016). *Structural Analysis and Design to Prevent Disproportionate Collapse*. USA: CRC Press. 978-1-4987-0680-3.
- Fu, F. (2018). *Design and Analysis of Tall and Complex Structures*. UK: Butterworth-Heinemann. 978-0-08-101121-8.
- Fu, F. (2021). *Fire Safety Design for Tall Buildings*. England: Taylor Francis. 978-0-367-44452-5.
- Guo, H., et al. (2004). Durability of recycled aggregate concrete—A review. *Cement and Concrete Composites*, 26(2), 97–98. [https://doi.org/10.1016/S0958-9465\(03\)00091-X](https://doi.org/10.1016/S0958-9465(03)00091-X)
- Hobbs, D. W. (1999). Aggregate influence on chloride ion diffusion into concrete. *Cement and Concrete Research*, 29(12), 1995–1998. [https://doi.org/10.1016/S0008-8846\(99\)00188-X](https://doi.org/10.1016/S0008-8846(99)00188-X)
- Huan, X. U. E., Zuquan, J. I. N., & Xiaojie, W. (2015). Chloride ion penetration into concrete exposed to marine environment for a long period. *The Ocean Engineering*, 33(5), 60–65. <https://doi.org/10.16483/j.jissn.1005-9865.2015.05.008>
- Ishida, T., Iqbal, P. O. N., & Anh, H. T. L. (2009). Modeling of chloride diffusivity coupled with non-linear binding capacity in sound and cracked concrete. *Cement and Concrete Research*, 39(10), 913–923. <https://doi.org/10.1016/j.cemconres.2009.07.014>
- Jung, S.-H., et al. (2018). Maintenance for repaired RC column exposed to chloride attack based on probability distribution of service life. *International Journal of Concrete Structures and Materials*, 12(1), 22. <https://doi.org/10.1186/s40069-018-0259-2>
- Kessler, S., et al. (2016). Effect of freeze–thaw damage on chloride ingress into concrete. *Materials and Structures*, 50(2), 121. <https://doi.org/10.1617/s11527-016-0984-4>
- Khanzadeh Moradillo, M., Shekarchi, M., & Hoseini, M. (2012). Time-dependent performance of concrete surface coatings in tidal zone of marine environment. *Construction and Building Materials*, 30, 198–205. <https://doi.org/10.1016/j.conbuildmat.2011.11.044>
- Khanzadeh-Moradillo, M., et al. (2015). Effect of wet curing duration on long-term performance of concrete in tidal zone of marine environment. *International Journal of Concrete Structures and Materials*, 9(4), 487–498. <https://doi.org/10.1007/s40069-015-0118-3>
- Li, D., Wang, X., & Li, L. (2019). An analytical solution for chloride diffusion in concrete with considering binding effect. *Ocean Engineering*, 191, 106549. <https://doi.org/10.1016/j.oceaneng.2019.106549>
- Liu, Y., & Weyers, R.E. (1998). Modeling the time-to-corrosion cracking in chloride contaminated reinforced concrete structures. *ACI Materials Journal* 95(6). <https://doi.org/10.14359/410>
- Marks, M., Glinicki, M. A., & Gibas, K. (2015). Prediction of the chloride resistance of concrete modified with high calcium fly ash using machine learning. *Materials*, 8(12), 8714–8727. <https://doi.org/10.3390/ma8125483>

- Meira, G. R., et al. (2007). Chloride penetration into concrete structures in the marine atmosphere zone—Relationship between deposition of chlorides on the wet candle and chlorides accumulated into concrete. *Cement and Concrete Composites*, 29(9), 667–676. <https://doi.org/10.1016/j.cemconcomp.2007.05.009>
- Mir, Z. M., et al. (2019). Enhanced predictive modelling of steel corrosion in concrete in submerged zone based on a dynamic activation approach. *International Journal of Concrete Structures and Materials*, 13(1), 11. <https://doi.org/10.1186/s40069-018-0321-0>
- Muthulingam, S., & Rao, B. N. (2014). Non-uniform time-to-corrosion initiation in steel reinforced concrete under chloride environment. *Corrosion Science*, 82, 304–315. <https://doi.org/10.1016/j.corsci.2014.01.023>
- Nogueira, C., Leonel, E., & Coda, H. (2012). Probabilistic failure modelling of reinforced concrete structures subjected to chloride penetration. *International Journal of Advanced Structural Engineering*, 4(1), 10. <https://doi.org/10.1186/2008-6695-4-10>
- Pack, S. W., et al. (2010). Prediction of time dependent chloride transport in concrete structures exposed to a marine environment. *Cement and Concrete Research*, 40(2), 302–312. <https://doi.org/10.1016/j.cemconres.2009.09.023>
- Pan, Z., Chen, A., & Ruan, X. (2015). Spatial variability of chloride and its influence on thickness of concrete cover: A two-dimensional mesoscopic numerical research. *Engineering Structures*, 95, 154–169. <https://doi.org/10.1016/j.engstruct.2015.03.061>
- Papakonstantinou, K. G., & Shinozuka, M. (2013). Probabilistic model for steel corrosion in reinforced concrete structures of large dimensions considering crack effects. *Engineering Structures*, 57, 306–326. <https://doi.org/10.1016/j.engstruct.2013.06.038>
- Petcherdchoo, A. (2015). Repairs by fly ash concrete to extend service life of chloride-exposed concrete structures considering environmental impacts. *Construction and Building Materials*, 98, 799–809. <https://doi.org/10.1016/j.conbuildmat.2015.08.120>
- Petcherdchoo, A., & Chindaprasit, P. (2019). Exponentially aging functions coupled with time-dependent chloride transport model for predicting service life of surface-treated concrete in tidal zone. *Cement and Concrete Research*, 120, 1–12. <https://doi.org/10.1016/j.cemconres.2019.03.009>
- Pillai, R. G., et al. (2019). Service life and life cycle assessment of reinforced concrete systems with limestone calcined clay cement (LC3). *Cement and Concrete Research*, 118, 111–119. <https://doi.org/10.1016/j.cemconres.2018.11.019>
- Poupard, O., et al. (2006). Corrosion damage diagnosis of a reinforced concrete beam after 40 years natural exposure in marine environment. *Cement and Concrete Research*, 36(3), 504–520. <https://doi.org/10.1016/j.cemconres.2005.11.004>
- Shaikh, F. U. A. (2018). Effect of cracking on corrosion of steel in concrete. *International Journal of Concrete Structures and Materials*, 12(1), 3. <https://doi.org/10.1186/s40069-018-0234-y>
- Song, H. W., et al. (2009). Service life prediction of repaired concrete structures under chloride environment using finite difference method. *Cement and Concrete Composites*, 31(2), 120–127. <https://doi.org/10.1016/j.cemconcomp.2008.11.002>
- Stambaugh, N. D., Bergman, T. L., & Srubar, W. V. (2018). Numerical service-life modeling of chloride-induced corrosion in recycled-aggregate concrete. *Construction and Building Materials*, 161, 236–245. <https://doi.org/10.1016/j.conbuildmat.2017.11.084>
- Stipanovic Oslakovic, I., Bjegovic, D., & Mikulic, D. (2010). Evaluation of service life design models on concrete structures exposed to marine environment. *Materials and Structures/Materiaux Et Constructions*, 43(10), 1397–1412. <https://doi.org/10.1617/s11527-010-9590-z>
- Sun, W., et al. (2002). Effect of chloride salt, freeze–thaw cycling and externally applied load on the performance of the concrete. *Cement and Concrete Research*, 32(12), 1859–1864. [https://doi.org/10.1016/S0008-8846\(02\)00769-X](https://doi.org/10.1016/S0008-8846(02)00769-X)
- Wang, Y., et al. (2018). Prediction model of long-term chloride diffusion into plain concrete considering the effect of the heterogeneity of materials exposed to marine tidal zone. *Construction and Building Materials*, 159, 297–315. <https://doi.org/10.1016/j.conbuildmat.2017.10.083>
- Wang, Y., Gong, X., & Wu, L. (2019). Prediction model of chloride diffusion in concrete considering the coupling effects of coarse aggregate and steel reinforcement exposed to marine tidal environment. *Construction and Building Materials*, 216, 40–57. <https://doi.org/10.1016/j.conbuildmat.2019.04.221>
- Xia, J., et al. (2019). Numerical simulation of steel corrosion in chloride contaminated concrete. *Construction and Building Materials*, 228, 116745. <https://doi.org/10.1016/j.conbuildmat.2019.116745>
- Xu, Q., Shi, D., & Shao, W. (2019). Service life prediction of RC square piles based on time-varying probability analysis. *Construction and Building Materials*, 227, 116824. <https://doi.org/10.1016/j.conbuildmat.2019.116824>
- Yang, L., Cai, R., & Yu, B. (2017). Formation mechanism and multi-factor model for surface chloride concentration of concrete in marine atmosphere zone. *Tumu Gongcheng Xuebao/china Civil Engineering Journal*, 50(12), 46–55. <https://doi.org/10.15951/j.tmgxcb.2017.12.006>
- Yang, L., Chen, C., & Yu, B. (2019). Multi-factor time-varying model of marine environmental action on concrete in splash zone. *Journal of the Chinese Ceramic Society*, 11(47), 1566–1572.
- Zeng, Y. (2007). Modeling of chloride diffusion in hetero-structured concretes by finite element method. *Cement and Concrete Composites*, 29(7), 559–565. <https://doi.org/10.1016/j.cemconcomp.2007.04.003>
- Zhang, K., et al. (2019). Analytical model for critical corrosion level of reinforcements to cause the cracking of concrete cover. *Construction and Building Materials*, 223, 185–197. <https://doi.org/10.1016/j.conbuildmat.2019.06.210>
- Zhao, Y., et al. (2016). Non-uniform distribution of a corrosion layer at a steel/concrete interface described by a Gaussian model. *Corrosion Science*, 112, 1–12. <https://doi.org/10.1016/j.corsci.2016.06.021>
- Zhao, Y., Hu, B., et al. (2011a). Non-uniform distribution of rust layer around steel bar in concrete. *Corrosion Science*, 53(12), 4300–4308. <https://doi.org/10.1016/j.corsci.2011.08.045>
- Zhao, Y., Karimi, A. R., et al. (2011b). Comparison of uniform and non-uniform corrosion induced damage in reinforced concrete based on a Gaussian description of the corrosion layer. *Corrosion Science*, 53(9), 2803–2814. <https://doi.org/10.1016/j.corsci.2011.05.017>
- Zheng, J. J., et al. (2018). A numerical algorithm for evaluating the chloride diffusion coefficient of concrete with crushed aggregates. *Construction and Building Materials*, 171, 977–983. <https://doi.org/10.1016/j.conbuildmat.2018.03.184>
- Zheng, J. J., Wong, H. S., & Buenfeld, N. R. (2009). Assessing the influence of ITZ on the steady-state chloride diffusivity of concrete using a numerical model. *Cement and Concrete Research*, 39(9), 805–813. <https://doi.org/10.1016/j.cemconres.2009.06.002>
- Zhu, X., & Zi, G. (2017). A 2D mechano-chemical model for the simulation of reinforcement corrosion and concrete damage. *Construction and Building Materials*, 137, 330–344. <https://doi.org/10.1016/j.conbuildmat.2017.01.103>

## Publisher's Note

Springer Nature remains neutral with regard to jurisdictional claims in published maps and institutional affiliations.

Submit your manuscript to a SpringerOpen® journal and benefit from:

- Convenient online submission
- Rigorous peer review
- Open access: articles freely available online
- High visibility within the field
- Retaining the copyright to your article

Submit your next manuscript at ► [springeropen.com](https://www.springeropen.com)